Journal of proteome research

Article

pubs.acs.org/jpr

# Apoe, Mbl2, and Psp Plasma Protein Levels Correlate with Diabetic Phenotype in NZO Mice—An Optimized Rapid Workflow for SRM-Based Quantification

Christine von Toerne,[†] Melanie Kahle,[‡,⊥] Alexander Schäfer,[†,⊥] Ruben Ispiryan,[§] Marcel Blindert,[†] Martin Hrabe De Angelis,[‡] Susanne Neschen,[‡] Marius Ueffing,[†,∥] and Stefanie M. Hauck*[,†]

[†]Research Unit Protein Science, [‡]Institute of Experimental Genetics, [§]Research Unit Scientific Computing, and [⊥]German Center for Diabetes Research (DZD), Helmholtz Zentrum München, German Research Center for Environmental Health (GmbH), Neuherberg, Germany

[∥]Centre of Ophthalmology, Institute for Ophthalmic Research, University of Tübingen, Tübingen, Germany

Supporting Information

**ABSTRACT:** Male New Zealand Obese (NZO) mice progress through pathophysiological stages similar to humans developing obesity-associated type 2 diabetes (T2D). The current challenge is to establish quantitative proteomics from small plasma sample amounts. We established an analytical workflow that facilitates a reproducible depletion of high-abundance proteins, has high throughput applicability, and allows absolute quantification of proteins from mouse plasma samples by LC−SRM-MS. The ProteoMiner equalizing technology was adjusted to the small sample amount, and reproducibility of the identifications was monitored by spike proteins. Based on the label-free relative quantification of proteins in depleted plasma of a test set of NZO mice, assays for potential candidates were designed for the setup of a targeted selected reaction monitoring (SRM) approach and absolute quantification. We could demonstrate that apolipoprotein E (Apoe), mannose-binding lectin 2 (Mbl2), and parotid secretory protein (Psp) are present at significantly different quantities in depleted plasma of diabetic NZO mice compared to non-diabetic controls using AQUA peptides. Quantification was validated for Mbl2 using the ELISA technology on non-depleted plasma. We conclude that the depletion technique is applicable to restricted sample amounts and suitable for the identification of T2D signatures in plasma.

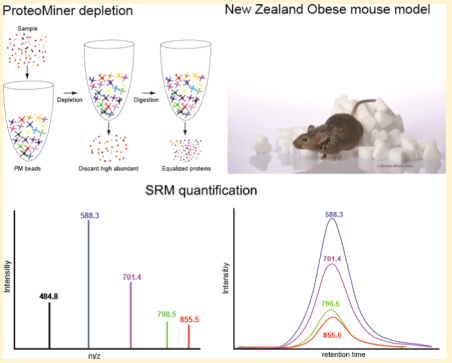


**KEYWORDS:** *type 2 diabetes, New Zealand Obese mouse, ProteoMiner, depletion, label-free quantification, selected reaction monitoring, absolute quantification, AQUA peptides, protein signatures*

## INTRODUCTION

The global spread of obesity and type 2 diabetes (T2D) poses immense challenges for health care systems worldwide.[1] T2D, typically associated with obesity and insulin resistance, is believed to develop partly as consequence of progressive dysfunction of insulin-secreting beta cells in the pancreas.[2] Various mechanisms have been proposed to initiate the pathophysiological process and contribute to beta cell failure.[2,3] Understanding these mechanisms is crucial for the development of dietary and pharmacological interventions that ultimately prevent and cure diabetes.[2] Animal models with a defined genetic background have been essential for the investigation of patho-mechanisms and to address hypothesis prior to clinical trials in humans. Furthermore, mouse models are very useful for benchmarking technologies since samples can be collected under standard operating protocols while food intake and behavior, as well as the onset and progression of disease, can be closely monitored in a well-defined experimental setting, thus allowing focusing on the variations associated with the technologies.[4]

The New Zealand Obese (NZO) mouse strain is a well-established polygenic model of morbid obesity.[5] In addition, NZO mice present many other characteristics of the human metabolic syndrome, such as insulin resistance and progression to overt diabetes associated with pancreatic beta cell degeneration,[5−10] hypercholesterolemia, and hypertension.[11] Male NZO spontaneously develop diabetes with a high frequency at an early age.[12] Since NZO mice resemble the human situation with respect to disease characteristics, they provide a suitable model for human obesity-associated type 2 diabetes (diabesity) and its secondary complications.[13,14] The NZO strain has previously been used for identification of mouse obesity and diabetes genes, and different genome-wide scans of outcross populations with lean strains have been performed.[15−19]

Plasma is the main clinical sample specimen and has long been acknowledged as an important source of information.

**Received:** October 19, 2012
**Published:** January 28, 2013

Table 1. Efficiency of ProteoMiner Depletion

| accession | peptides used for quantification | depletion in % | gene symbol | description |
|---|---|---|---|---|
| ENSMUSP00000031314 | 65 | 97 | Alb | albumin gene |
| ENSMUSP00000035158 | 35 | 96 | Trf | transferrin gene |
| ENSMUSP00000033185 | 20 | 98 | Hpx | hemopexin gene |
| ENSMUSP00000042095 | 13 | 75 | Serpina3k | serine (or cysteine) peptidase inhibitor, clade A, member 3K gene |
| ENSMUSP00000003714 | 10 | 63 | Cp | ceruloplasmin gene |
| ENSMUSP00000023583 | 9 | 75 | Ahsg | alpha-2-HS-glycoprotein gene |
| ENSMUSP00000000049 | 9 | 60 | Apoh | apolipoprotein H gene |
| ENSMUSP00000074436 | 6 | 95 | Hp | haptoglobin gene |
| ENSMUSP00000072652 | 5 | 88 | Serpina 1a | serine (or cysteine) peptidase inhibitor, clade A, member 1A gene |
| ENSMUSP00000077909 | 5 | 98 | Serpina 1d | serine (or cysteine) peptidase inhibitor, clade A, member 1D gene |
| ENSMUSP00000023587 | 5 | 99 | Fetub | fetuin beta gene |
| ENSMUSP00000111003 | 2 | 93 | Kng 1 | kininogen 1 gene |
| ENSMUSP00000034189 | 2 | 93 | Ces 1c | carboxylesterase 1C gene |

However, this complex sample poses major challenges for proteomic analysis.[20,21] The unique combination of a very high complexity with proteins that vary in quantity by more than 10 orders of magnitude has to be overcome.[20] Depletion of very high abundant proteins is mandatory before plasma samples become applicable for shotgun proteomics. Previous studies have demonstrated that a reasonable analytical depth after depletion can be achieved.[22] Even so, these approaches require large amounts of plasma per individual as starting material. In the era of biobanking initiatives and genome-wide association studies facilitating the discovery of risk factors and genotype-phenotype correlations, a workflow for acquiring quantitative proteomic data from limited plasma sample volumes is necessary to complement genomic data from large cohorts with targeted or non-targeted proteomic signatures. In order to address this need, we adapted the taxonomy-independent ProteoMiner (Bio-Rad) depletion approach to small starting amounts of plasma featuring reproducible depletion and high throughput applicability (Table 1). The ProteoMiner protein enrichment technology employs a large, highly diverse bead-based library of combinatorial peptide ligands. When added to a complex sample such as plasma, highly abundant proteins saturate their high-affinity ligands and can be depleted during extensive washing, while lower abundant proteins are concentrated on their specific affinity ligands. Therefore, unlike other bead-based or immuno-based depletion techniques, depletion is reached by discarding the unbound protein (supernatant) and proceeding with the bead-bound fraction.

As a proof of principle, we employed this workflow on plasma from the NZO mouse model for T2D, investigating phenotype-associated protein signatures using absolute quantification by selected reaction monitoring mass spectrometry (LC−SRM-MS). Using a test set of diabetic (diab) and non-diabetic (nd) NZO mice, candidate proteins were identified by label-free quantification of shotgun LC−MS/MS data. These candidates were further evaluated in a semiquantitative selected reaction monitoring (SQ-SRM) approach, on an extended set of animals. Finally, candidate proteins were identified that allow a significant discrimination between disease phenotypes as selected by principal component analysis. These candidates were re-analyzed by SRM-based absolute quantification (Q-SRM) using the AQUA approach according to the method of Gerber et al.[23] and confirmed for one candidate by ELISA technology on non-depleted plasma.

## MATERIALS AND METHODS

### Animals

All animals were bred in house and housed in isolated ventilated cages (IVC-Racks, BioZone) supplied with filtered air, in a 12/12 h light/dark cycle (lights on from 6 a.m. until 6 p.m.). To determine changes in the plasma proteome independent of dietary factors in the diabetic versus non-diabetic state, NZO males were fed with pro-diabetogenic diets with either high or low amount of fat after weaning at an age of 3 weeks. Diets and water were available ad libitum. The allocation of the animal into the groups "diabetic", "moderate diabetic", and "non-diabetic" was based on the following physiological parameters: elevated blood glucose levels, polyuria and polydipsia, as well as loss or stagnation of bodyweight. In our definition blood glucose levels of over 400 mg/dL and a bodyweight loss or stagnation for a period of over 3 weeks was considered to indicate a diabetic condition. Twenty-three NZO males with a body weight mean of 51 ± 2 g were considered overtly diabetic and displayed severe hyperglycemia with a mean random fed plasma glucose concentration of 855 ± 21 mg/dL accompanied by a low mean plasma insulin concentration of 1.5 ± 0.3 $\mu$g/L, suggesting pancreatic $\beta$-cell atrophy. A second group of 13 NZO males with mean body weight of 69 ± 2 g was considered non-diabetic and displayed a mean random fed plasma glucose concentration of 344 ± 19 mg/dL compensated by high mean plasma insulin concentrations of 13.7 ± 2.4 $\mu$g/L. A third small group of 4 male mice with a body weight mean of 71 ± 5 g showed an intermediary diabetic phenotype (termed "moderately diabetic") exhibiting a mean plasma glucose concentration of 501 ± 58 mg/dL. Upon sacrifice the age of overtly diabetic mice ranged between 14 and 49 weeks (mean age 22 weeks), of non-diabetic controls between 16 and 39 weeks (mean age 22 weeks), and of moderately diabetic individuals between 21 and 43 weeks (mean age 31 weeks). A varying of age of animals was allowed to exclude observation of changes in the proteome to be solely age-dependent. The different group sizes are a result of male NZO mice to spontaneously develop diabetes at a high frequency, with a bias in animal numbers toward the diabetic group. *In vivo* experiments were conducted in the German Mouse Clinic phenotyping platform (GMC).[24,25] Concentration values are displayed as means ± SEM. All values are summarized in Supplementary Table S1. All procedures for animal handling and experiments were performed in accordance with protocols approved by the local state authority


dx.doi.org/10.1021/pr3009836 | J. Proteome Res. 2013, 12, 1331−1343

Table 2. Candidates Selected for SRM Development

| accession | peptides used for quantification | ratio diab vs nd | gene symbol | description |
|---|---|---|---|---|
| ENSMUSP00000034585 | 13 | 1.9 | Apoa4 | apolipoprotein A-IV gene |
| ENSMUSP00000036044 | 44 | 0.7 | Apob | apolipoprotein B gene |
| ENSMUSP00000003066 | 9 | 0.7 | Apoe | apolipoprotein E gene |
| ENSMUSP00000025249 | 2 | 1.5 | Apom | apolipoprotein M gene |
| ENSMUSP00000024988 | 32 | 0.5 | C3 | complement component 3 gene |
| ENSMUSP00000022616 | 11 | 1.5 | Clu | clusterin gene |
| ENSMUSP00000028239 | 12 | 0.3 | Gsn | gelsolin gene |
| ENSMUSP00000028233 | 13 | 0.3 | Hc | hemolytic complement gene |
| ENSMUSP00000126449 | 20 | 0.6 | Itih1 | interalpha trypsin inhibitor, heavy chain 1 gene |
| ENSMUSP00000006703 | 15 | 0.4 | Itih4 | inter alpha-trypsin inhibitor, heavy chain 4 gene |
| ENSMUSP00000025797 | 6 | 2.0 | Mbl2 | mannose-binding lectin (protein C) 2 gene |
| ENSMUSP00000061519 | 5 | 0.5 | Pltp | phospholipid transfer protein gene |
| ENSMUSP00000046080 | 3 | 8.7 | Psp | parotid secretory protein gene |

(District Government of Upper Bavaria, Regierung von Oberbayern, Az 55.2-1-54-2531-113-08).

## Plasma Samples

Terminal *Vena cava* blood samples were withdrawn in EDTA-coated syringes between 8 and 10 a.m. (S-Monovette, 1.2 mL, K3E and S-Monovette-canula 22G × 1-1/2″, Sarstedt, Germany). Blood was centrifuged, and EDTA plasma aliquots were shock frozen in liquid nitrogen and stored at −80 °C until further processing. To ensure an unbiased analysis, all samples were blinded, and numbers were assigned prior to sample processing, mass spectrometric analysis, and ELISA quantification. Plasma glucose concentrations were determined with a glucometer (Olympus AU 480, Beckman Coulter) and plasma insulin concentrations with a commercial ELISA kit according to the manufacturer's instructions (Cat. 10-1247-01, Mercodia).

## Plasma Depletion Using ProteoMiner Beads

The ProteoMiner (Bio-Rad) beads were obtained as dry bulk beads (Cat. 163-3012, Bio-Rad). Beads were applied in batch mode as 20% slurry. For activation, beads were washed three times with ice-cold 1x TBS (30 mM Tris, 150 mM NaCl, pH 7.8). In parallel, a spike proteins master-mix was prepared in ice-cold 1x TBS, adding ribulose-1,5-bisphosphate carboxylase oxygenase (Sigma), yeast alcohol dehydrogenase 1 (Sigma), and bovine lactoglobulin (Sigma) to a final amount of 50 fmol per sample. Plasma samples were thawed on ice and centrifuged at 12,000 rpm for 1 min at 4 °C, and 10 μL of plasma was transferred to LoBind tubes (Eppendorf). The 10 μL of washed beads per sample was mixed with spike proteins, filled up to 500 μL per sample with ice-cold 1x TBS, and combined with the plasma samples. Samples and beads were allowed to incubate rotating overhead at medium speed for 3 h at 4 °C. Subsequently, samples were centrifuged for 30 s at 1000*g* at 4 °C. Proteins bound to the beads (equalized proteins) were collected, and the supernatants containing the unbound, highly abundant proteins were removed. The ProteoMiner beads containing the bound proteins were washed three times with ice-cold 1x TBS.

## On-Bead Digestion with Trypsin

Proteins bound to the beads were reduced by addition of dithiothreitol (DTT) to a final concentration of 100 mM and incubated at 60 °C for 15 min (min). Cysteines were then alkylated with iodacetamide (Merck) at a final concentration of 300 mM for 30 min at room temperature in the dark. Samples were digested using 1 μg trypsin (Sigma) in 1x TBS at 37 °C overnight with gentle shaking. After digestion, samples were adjusted to a volume of 100 μL using 1x TBS and centrifuged at 3000*g* for 1 min, and supernatants were stored at −20 °C until further use.

## Non-targeted LC–MS/MS

For the non-targeted label-free quantification, depleted plasma from the test set of NZO mice was analyzed (5 diabetic, 2 moderately diabetic, and 4 non-diabetic mice). Prior to the LC–MS/MS analysis, the digested samples were diluted 5-fold in 2% acetonitrile/0.5% trifluoroacetic acid (TFA) and centrifuged for 5 min at 4 °C before loading. LC–MS/MS analysis was performed as described previously on a LTQ-Orbitrap XL (Thermo Scientific).[26] Briefly, peptides were trapped on a nano trap column (300 μm i.d. × 5 mm, packed with Acclaim PepMap100 C18, 5 μm/100 Å; LC Packings) in 0.1% TFA at a flow rate of 30 μL/min for 5 min before separation by reversed phase chromatography (PepMap,15 cm,75 μm i.d., 3 μm/100 Å pore size, LC Packings) operated on a nano-HPLC (Ultimate 3000, Dionex) with a nonlinear 170 min gradient using 2% acetonitrile in 0.1% formic acid in water (A) and 0.1% formic acid in 98% acetonitrile (B) at a flow rate of 300 nL/min. The gradient settings were 5–140 min, 2–31% B; 140–145 min, 31–95% B; 145–150 min, 95% B and followed by equilibration for 15 min to starting conditions. From the MS prescan (acquired in profile mode), the 10 most abundant peptide ions were selected for fragmentation in the linear ion trap if they exceeded an intensity of at least 200 counts and if they were at least doubly charged. Dynamic exclusion was set to 30 s. During fragment analysis a high-resolution (60,000 fwhm) MS spectrum was acquired in the Orbitrap with a mass range from 300 to 1500 Da.

## Protein Identification and Label-Free Relative Quantification

The RAW files from the test set (Thermo Xcalibur file format) were further analyzed using the Progenesis LC–MS software (version 4.0, Nonlinear) as described previously.[26] Briefly, the profile data of the MS scans and MS/MS spectra were imported and transformed to peak lists with Progenesis LC–MS using a proprietary algorithm and stored in peak lists comprising $m/z$ and abundance. One sample was set as reference. The retention times of all other samples within the experiment were aligned (3–5 manual landmarks, followed by automatic alignment) to create maximal overlay of the two-dimensional feature maps. Features with one charge or ≥8 charges were masked and excluded from further analyses. All remaining features were


dx.doi.org/10.1021/pr3009836 | J. Proteome Res. 2013, 12, 1331–1343

used to calculate a normalization factor for each sample that corrects for experimental variation. Samples were allocated to their experimental group (diab, md, nd). For peptide identification, Mascot (Matrix Science, version 2.3) was set up to search with one missed cleavage allowed, a fragment ion mass tolerance of 0.6 Da, and a parent ion tolerance of 10 ppm. Carbamidomethylation was set as fixed modification, and methionine oxidation and asparagine or glutamine deamidation were allowed as variable modifications. Spectra were searched against the Ensembl mouse database (Release 62; 54576 sequences), and a Mascot-integrated decoy database search calculated an average peptide false discovery rate of <2% when searches were performed with an ion score cutoff of 30 and a significance threshold of $p < 0.01$. Peptide assignments were reimported into Progenesis LC−MS. Normalized abundances of all unique peptides were summed up and allocated to the respective protein. Proteins with less than 2 peptides used for quantification were excluded. Maximum fold changes were calculated by the software between the averaged abundances of the three conditions non-diabetic, diabetic, and moderately diabetic for every protein. Proteins with fold changes of ≥1.4 were considered to be potentially differential between the different groups (Table 2 and Supplementary Table S2). For 13 of these candidates SRM assays were generated (Supplementary Table S3).

### Peptide Selection and Development of SRM Assays

For the setup of SRM assays, the shotgun data from depleted mouse plasma samples were used to empirically select transitions meeting the SRM peptide criteria (Supplementary Table S10). The Scaffold software (version 3_00_03, Proteome Software Inc.) was used to validate MS/MS-based peptide identifications and spectra as basis for developing SRM assays (Supplementary Tables 2 and 10). Peptide identifications were accepted if they could be established at greater than 80% probability as specified by the Peptide Prophet algorithm.[27] Proteotypic peptides for SRM assays were selected from peptides identified in all samples, without variable modifications, a Mascot score above 30, good ion statistics, and avoiding amino acids methionine, tryptophan, and cysteine.

SRM transitions of proteotypic peptides were evaluated using the MRMPilot software (version 2.0, AB SCIEX). First, Mascot DAT files containing annotated MS/MS spectra were loaded into the program. Next, the seven highest y-ions for up to 3 peptides per protein were selected from the DAT files to create SRM assays. Collision energy was calculated based on the precursor charge state and mass-to-charge ratio using the standard equation of the software $CE = 0.03m/z + 2.905$ and $CE = 0.038m/z + 2.281$ for doubly and triply charged precursors, respectively. After data acquisition on the QTrap4000 (AB SCIEX), only those peptides were kept that showed a clear difference between signal and background noise, coelution of at least 4 transitions, as well as MS/MS verification. In cases without MS/MS verification, crude peptides (JPT-Innovative Peptide Solutions) were purchased for MS/MS verification and SRM optimization. Collision energy (CE) optimization was performed on fragment ions using a range of −5 to +5 V around the calculated CE value in steps of 1 V, and collision cell exit potential optimization was performed on fragment ions using a range of 11−18 V in steps of 1 V.

### Targeted Mass Spectrometry

Prior to LC−MS/MS analysis, the digested samples were diluted 5-fold in 2% acetonitrile/0.5% TFA and centrifuged for 5 min at 4 °C before loading 10 μL. LC−MS/MS analysis for the targeted approach was performed on a Tempo nano MDLC system (Eksigent) coupled online to a QTrap4000 (AB SCIEX) mass spectrometer by a nano spray ion source. Peptides were trapped on a nano trap column (300 μm i.d. × 5 mm, packed with Acclaim PepMap100 C18, 5 μm, 100 Å; LC Packings) in 0.1% TFA at a flow rate of 20 μL/min for 5 min and separated on an analytical column (75 μm i.d. × 15 cm, Acclaim PepMap C18, 3 μm, 100 Å, nanoViper; LC Packings) by a 90 min nonlinear gradient using 2% acetonitrile in 0.1% formic acid in water (A) and 0.1% formic acid in 98% acetonitrile (B) at a flow rate of 250 nL/min. The gradient settings were 5−65 min, 5−45% B; 65−70 min, 45−90% B; 70−72 min, 90% B; 72−80 min, 90−5% B, followed by re-equilibration for 10 min to starting conditions. The MS was used in positive ion mode with 2600 V ion spray voltage, curtain gas setting of 14, ion source gas setting of 30, nebulizer gas setting of 0, and an interface heater temperature of 170 °C. Eluted peptides were measured with a scheduled SRM method in a SRM detection window of 360 s and a target scan time of 3 s. The resolution in Q1 and Q3 was set to unit (0.7 amu fwhm).

### Semiquantitative SRM (SQ-SRM)

For SQ-SRM, data generated from 35 animals were loaded into the MultiQuant software (Version 1.2, AB SCIEX). Settings of the integration defaults were MQL integration algorithm, Gaussian smooth width at 3 points, retention time half window 90 s, minimum peak width 3 points, minimum peak height 20, noise percentage 40%, baseline subtractions window 2 min, peak splitting factor 4 points. Quality of signals and correct annotation of peaks were curated by hand to ensure proper peak integration and retention time alignment of multiple transitions emanating from each peptide. Only transitions showing consistency across runs with a signal-to-noise ratio >12 were included in the analysis. Quantification relevant information was exported to Microsoft Excel 2010 for further calculations (Supplementary Table S3). In the semiquantitative SRM approach, the relative quantification was based on the area under the curve (AUC) values, the peak areas of the transitions. Since the peak area varies strongly between the different transitions of one peptide, all absolute peak area values were transformed into a percent variation for better comparability between samples. To this end, the peak area of each transition was divided by the average peak area of all samples, creating a ratio for every transition. The four measured transition ratios of every peptide were controlled for coherence and then averaged, creating a peptide ratio. These peptide ratios were further averaged between the 2−3 peptides measured per protein, creating a protein ratio for every sample and thus building the basis for the comparison between the different animals. Data was normalized against the protein ratios of all three spike proteins, averaged per animal. The averaged spike protein ratios are referred to as individual spike factors throughout this document.

### Absolute Quantification by SRM (Q-SRM)

Absolute quantification was performed using the AQUA approach according to the method of Gerber et al.[23] on the depleted plasma of the complete set of 40 NZO mice. Each of the three proteins Apoe, Mbl2, and Psp was quantified against

two heavy peptides (Supplementary Tables S7 and S9). For MS/MS confirmation of sequences of the SRM assays of the heavy peptides acquired on the QTrap4000 (MS/MS confirmation of label-free results are reported in Supplementary Table 10) the Scaffold software (version 3_00_03, Proteome Software Inc.) was used. Supplementary Figure 2 displays the MS/MS spectra of the six heavy peptides used for absolute quantification.

Prior to implementing quantitative assays, key parameters characterizing the analytical performance of the assays were determined for measurement in plasma samples, following the study of Whiteaker et al.[4] To this end, we calculated the linear range of the assays (Supplementary Figure 3), the limits of detection (LOD) and limits of quantification (LOQ) (Supplementary Table S8 and Supplementary Figure 3), and the precision of the measurement of the assay (Supplementary Table S6). A response curve of the heavy peptides was generated in depleted and digested plasma. Three technical repeats were performed at nine concentration points, complemented by blanks and double blank runs. First order polynomial regression was used to fit the serial dilution data points for each curve, using a 1/y weighting on all points having a correlation coefficient of >0.99 (Prism software, version 5, GraphPad). Precision was determined by measuring the CV in percent. Additionally, the variation of concentration points nearest the calculated LOQ must be <30%. LOD and LOQ for each target were obtained by using the average of the three blank measurements plus three times the standard deviation of the noise (for LOD) and ten times the standard deviation of the noise (for LOQ), respectively (Supplementary Table S8).

On the basis of the previous relative quantification of Apoe, Mbl2, and Psp, concentrations of heavy peptides were spiked at the level of approximate endogenous concentrations of the respective analytes to ensure the maximum linear dynamic range of the SRM assays.[28] For absolute quantification, 40 fmol for Apoe and Mbl2 peptides and 2 fmol for Psp peptides was added to each sample directly before the LC−MS/MS analysis to avoid losses of heavy peptides during sample processing steps, thereby ensuring an accurate quantification. The absolute quantification is based on the ratio between the heavy peptides to the light (endogenous) peptides of unknown concentration. Heavy to light ratios for each transition were determined using the MultiQuant software (Version 1.2, AB SCIEX), applying the same settings as for the relative quantification approach. Quantification relevant information was exported to Microsoft Excel 2010 for further calculations. Individual spike factors were calculated for every sample.

### Enzyme Linked Immunosorbent Assay

Measurement of the Mbl2 concentration in non-depleted plasma was performed using the mouse Mbl2 DuoSet ELISA development system (R&D Systems) according to manufacturer's instructions. The Mbl2 ELISA was first tested on the non-depleted plasma samples from the test set of animals to identify necessary dilutions of diabetic and non-diabetic samples. On the basis of these results, all samples were measured in a final dilution of 1:15000, performed in two dilution steps. For the final experiments, 38 (23 diabetic, 12 non-diabetic, and 3 moderately diabetic) of the original plasma samples used for the mass spectrometric analysis were measured.

### Statistical Analyses

Protein distributions for the diabetic, non-diabetic, and moderately diabetic groups were plotted, and two-sided Wilcoxon rank sum tests were carried out to test for differences between the medians of the groups based on the relative SRM quantification. A principal component analysis (PCA) using the technique of multiple analyses of variances (MANOVA) for animal groups was carried out. We also performed a dimension reduction (feature selection) based on PCA. The visualization graphs, hypothesis tests, and PCAs were performed using the software MATLAB, version R2010. For absolute quantifications and the ELISA data, a non-parametric analysis of variance (ANOVA) was performed comparing the animal groups with the Kruskal−Wallis test, followed by Dunn's post-test, correcting for multiple testing (Prism software, version 5, Graphpad). *P*-values less than 0.05 were considered to indicate statistically significant differences.

## RESULTS

### Development of a Rapid Depletion Workflow for Small Plasma Volumes

Since plasma samples from small animal studies and human biobanks are limited and often only very small volumes are available, it is crucial to develop a workflow that facilitates analysis of protein signatures using minimal amounts of starting material.

To develop a scalable and species-independent workflow, we adapted the ProteoMiner (PM) enrichment technology, which was reported to demonstrate broad binding capacity of low abundant proteins while removing high abundant proteins.[29−31] The main challenge for plasma proteomics with small amounts of starting material is the limited analytical depth, resulting in a limited number of identified proteins. Therefore we first challenged the workflow with reduction of sample input (data not shown). Amounts ranging from 10 to 50 $\mu$L human and mouse plasma samples were used, which corresponds to the typical amounts available from, e.g., human cohort plasma collections. Within this range, a comparable number of proteins were identified (data not shown). Therefore, the protocol was further optimized for plasma volumes of 10 $\mu$L. As the reproducibility of our simple and rapid depletion protocol is a crucial factor, we assessed the reproducibility of all tested workflows by label-free quantification of protein abundances based on peak intensities as described before.[26,32] With respect to reproducibility, the batch application of beads outperformed the column-based approach (data not shown). The usage of low protein binding consumables greatly increased the performance of the workflow (data not shown). Following plasma depletion, gel-free on-bead digestion demonstrated the highest efficiency and reliability. Using our established protocol, we finally compared the performance of the PM beads to two sets of silica-coated superparamagnetic beats (BcMag Hydroxyapatite and BcMag PSA, Bioclone Inc.). The PM beads outperformed the other tested beads with respect to handling, protein identification, and reproducibility (data not shown).

Any depletion protocol has to be assessed for efficacy with respect to depletion of high abundant plasma proteins. To this end, we quantified protein abundances of depleted plasma samples in comparison to crude plasma, using the label-free approach. We observed a depletion efficiency of more than 60% for 13 different high abundant plasma proteins, including albumin, transferrin and haptoglobin (Table 1; a detailed list of

all abundances in crude and depleted plasma is given in Supplemental Table 11).

## Reproducibility of the Depletion Workflow

After optimization of the depletion protocol for 10 $\mu$L plasma samples, we assessed the technical reproducibility (TR) of the SRM approach, with respect to high-throughput applicability. As a first step, we calculated the technical variability of the targeted mass spectrometric measurement by repeatedly (10 repetitions) measuring our 13 candidate proteins in pooled plasma from NZO mice. The median CV of the technical variability of the measurements was 5.5% (Figure 1A and Supplementary Table S4). This graphical analysis of the TR shows the transition with the highest variability between replicates. It originated from a peptide of the complement factor C3, which we did not pursue for the absolute quantification. This optical quality control allows for proteins below a certain quality of detection to be selected and excluded from further analysis. To expand this analysis of variability to cover the optimized sample workflow (including depletion and protein digestion in addition to mass spectrometry measurement), we processed 10 identical aliquots from one plasma sample in parallel. The median CV of this interassay variability for the 13 SQ-SRM assays was 16% (Figure 1B and Supplementary Table S5). Our data is comparable to the performance of the current state-of-the-art LC−MS and SRM assay.[33]

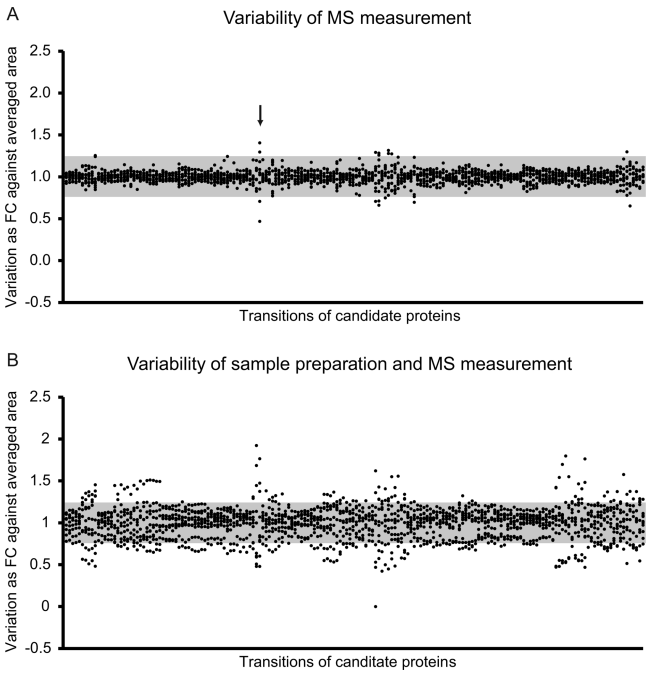


**Figure 1.** Variability of MS measurement and ProteoMiner sample preparation. Reproducibility of the Tempo nano MDLC system (Eksigent) coupled online to a QTrap4000 (AB SCIEX) mass spectrometer by a nano spray ion source was assessed. Repeated measurements of one NZO plasma (depleted) sample for 10 times using the SQ-SRM method for 13 candidate proteins (A). The median coefficient of variation was calculated to be 5.5%. Panel A displays the technical variability for the 180 measured transitions ($x$-axis) as fold changes of single peak areas divided by the peak areas averaged through the 10 replicates ($y$-axis). The arrow indicates the transition with the largest variability between the 10 replicates. The median coefficient of variation induced through the sample preparation process (including ProteoMiner depletion, digestion, and mass spectrometric measurement) was estimated to be 16% (B). Displayed are the combined variations for 180 measured transitions ($x$-axis) as fold changes of single peak areas divided by the peak areas averaged through the 10 replicates ($y$-axis). The gray bars mark the ±25% variation.

Although the inter-assay variability was very low (CV 16%), we implemented additional controls to evaluate variations between different depleted samples. For that reason, all samples were spiked with a set of proteins from a non-rodent origin. Spike proteins ranged in molecular weights to exclude a bias between protein mass and depletion efficiency. Spiking of these proteins was performed prior to sample preparation procedure and thus allowed to monitor all irregularities during depletion and digestion, as well as variation in mass spectrometric measurements. Based on the spike proteins, a so-called "spike factor" was determined for every individual sample that facilitated the normalization across samples.

## Detection of Differentially Expressed Proteins in Plasma by Shotgun Proteomics

As a proof of principle we applied our depletion workflow for the analyses of protein signatures in plasma of a T2D mouse model. To preselect candidate proteins that could differ in abundance between diabetic and non-diabetic animals, a label-free relative quantification was performed. For these analyses we used shotgun LC−MS/MS data from depleted plasma of a test set of NZO mice including 4 non-diabetic, 5 diabetic, and 2 moderately diabetic mice. A total of 126 proteins were identified with 91 proteins identified by more than one peptide. Only proteins quantified with at least two peptides were considered for further analysis (Supplementary Table 2). Proteins demonstrating a ratio between the diabetic and the non-diabetic of $\geq$1.4 or $\leq$0.7 were considered potentially relevant, and a set of 13 proteins was chosen for the development of SRM assays (Table 2).

## Statistical Evaluation of Candidates by SQ-SRM

Expression levels of potential candidates identified by the shotgun approach were further studied using a semiquantitative, targeted SRM approach (SQ-SRM) on a larger set of animals (35 animals). SRM assays were recorded for 13 candidate and 3 spike proteins on 22 diabetic, 9 non-diabetic, and 4 moderately diabetic male NZO mice. Relative quantification was based on the AUC values, normalized against the spike factor (see also Semiquantitative SRM). The fold changes ranged from 0.2 to 4.2 comparing peak areas of single animals with the average transition (Figure 2). On the basis of the SQ-SRM data, we selected the best candidates according to their ability to discriminate between the biological groups for absolute quantification. The analysis of data distribution demonstrated the highest significance in group differences among the set of 13 candidates for Mbl2, Apoe, and Psp (Supplementary Figure 1). Following the analysis of group differences, we performed a MANOVA by obtaining principal components for all group means (Figure 3). All three animal groups can be clearly separated on the basis of the principle component analysis of the SQ-SRM results (Figure 3A). Then, we sorted the proteins according to their shares in principal components as follows. The coefficients of the variables (proteins) that generate principal components, often referred to as loadings, were used. The modules of loadings were scaled by values of explained variability of the corresponding principal component. Further sorting in descending order provides the list of proteins


dx.doi.org/10.1021/pr3009836 | J. Proteome Res. 2013, 12, 1331−1343

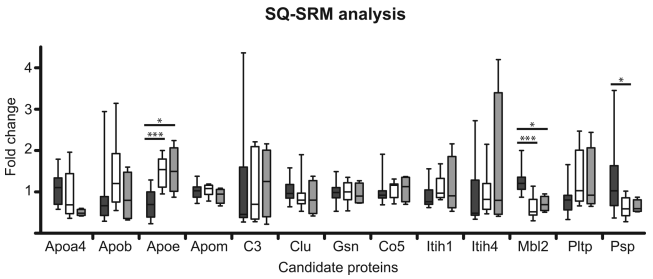


**Figure 2.** SQ-SRM results. For the SQ-SRM approach peptides from 13 candidate proteins were measured in depleted plasma from 35 NZO mice by LC−SRM-MS. Normalized protein ratios were calculated on the basis of these SRM measurements and then averaged within the experimental groups (diabetic, dark gray; non-diabetic, white; and moderately diabetic, light gray). The averaged protein ratios are displayed as boxplots. A non-parametric ANOVA was performed comparing the animal groups with the Kruskal−Wallis test, followed by Dunn's post-test, correcting for multiple testing. The ANOVA demonstrated a statistical significance between the diabetic and the non-diabetic groups for Apoe, Mbl2, and Psp, as well as a statistical significance between the non-diabetic and the moderately diabetic animals for Apoe and Mbl2.

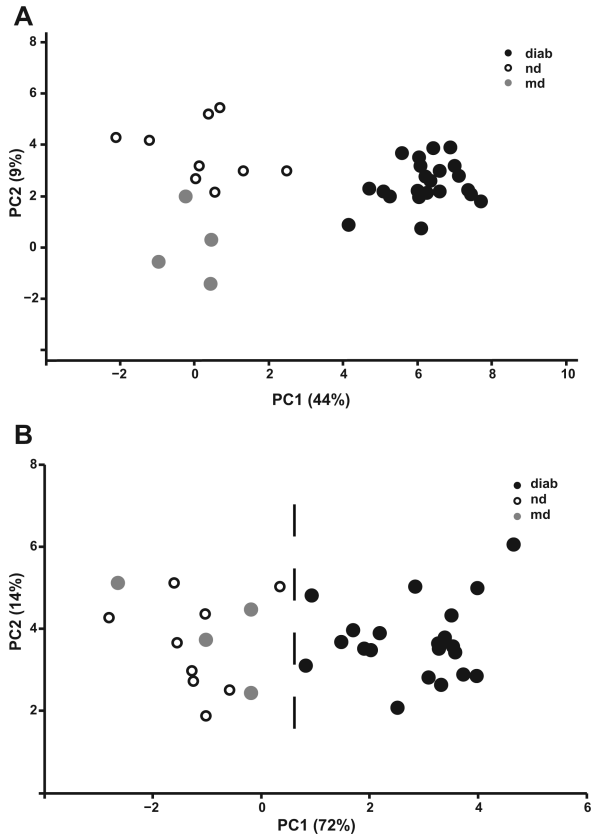


**Figure 3.** Identification of differential candidates by principle component analysis. Multivariate analysis of variance (MANOVA) based principle component analysis (PCA) was performed on the targeted, SRM-based relative quantifications of 13 proteins in 35 animals to identify the candidates with the most variance between the diabetic and non-diabetic groups. A clear separation of all three animal groups was observed, based on the 13 proteins investigated by SRM (A). The PCA analysis of only the three proteins Apoe, Mbl2, and Psp shows that the diabetic group can still be separated from the non-diabetic and moderately diabetic groups (B).

according to their importance in variance of animal groups. In simple terms, the proteins were sorted according to their share in the separation of groups, diabetic, non-diabetic, and moderately diabetic. A biased sequence of proteins was constructed, based on the results of the group-difference tests and the MANOVA/PCA. Mbl2 and Apoe were the first two proteins on this sorted list, followed by Psp. Although the initial 13 candidates stratify all three experimental groups, discrimination between diabetic and non-diabetic animal could still be achieved based solely on Mbl2, Apoe, and Psp (Figure 3B). On the basis of these results, Apoe, Mbl2 and Psp were chosen for absolute quantification in plasma samples.

## Absolute Quantification of Apoe, Mbl2, and Psp in Depleted Plasma Samples

Absolute quantification was obtained for the three statistically most significant proteins Apoe, Mbl2, and Psp, identified in the targeted relative quantification approach (SQ-SRM), using the AQUA approach.[23] Absolute quantity of proteins was determined via the ratios of heavy (AQUA) and light (endogenous) peptides. For each protein, two different and unique AQUA peptides were chosen (Supplementary Figure 2). To characterize key analytical parameters of our assay, we performed spike experiments of heavy peptides into plasma samples. Response curves with varying heavy peptide concentrations and constant endogenous light peptide were generated to calculate the linear range of the assays, the LOD, LOQ, and the precision of the assay (Supplementary Tables S6 and S8, Supplementary Figure 3). The responses were linear over 3−4 orders of magnitude for all peptides (Supplementary Figure 3). The median CV across all concentration points and across all analytes was 4.4%. The median LOD of our assays was 104 amol peptide (on column, measured in plasma, assuming complete trypsin digestion and molar stoichiometry between peptide and protein) and the median LOQ was 165 amol peptide (on column), ranging from 143 to 932 amol. All measured values are well within the expectation according to machine performance and are compare to published data.[4,33]

Mean Apoe concentrations in depleted plasma were determined to be 265 fmol/$\mu$L (53 fmol on column) in the diabetic, 539 fmol/$\mu$L (108 fmol on column) in the non-diabetic, and 629 fmol/$\mu$L (126 fmol on column) in the moderately diabetic group. Non-parametric ANOVA analysis followed by a post-test correction for multiple analyses revealed a high statistical significant difference between the diabetics and the non-diabetics ($p < 0.001$). In addition, a statistically significant difference between the non-diabetic and the moderately diabetic animals ($p < 0.05$) was readily detectable (Figure 4A). With respect to the moderately diabetic group, we want to draw attention to the fact that statistics allows calculations of statistical significance on groups of four animals, but interpretations of these results have to be made cautiously. Mean Mbl2 concentrations in depleted plasma of 355 fmol/$\mu$L (71 fmol on column) in the diabetic mice were significantly difference from non-diabetic (170 fmol/$\mu$l34 fmol on column, $p < 0.001$), and moderately diabetic group (221 fmol/$\mu$L 44 fmol on column; $p < 0.05$) (Figure 4B). Psp concentrations in depleted plasma were in the low femtomolar range, which makes this protein less abundant than Apoe and Mbl2 by approximately 100-fold. Mean Psp was measured to be on average 17 fmol/$\mu$L (3.6 fmol on column) in the diabetic, 3.1 fmol/$\mu$L (0.63 fmol on column) in the non-diabetic, and 4.3 fmol/$\mu$L (0.86 fmol on column) in the moderately diabetic


dx.doi.org/10.1021/pr3009836 | J. Proteome Res. 2013, 12, 1331−1343

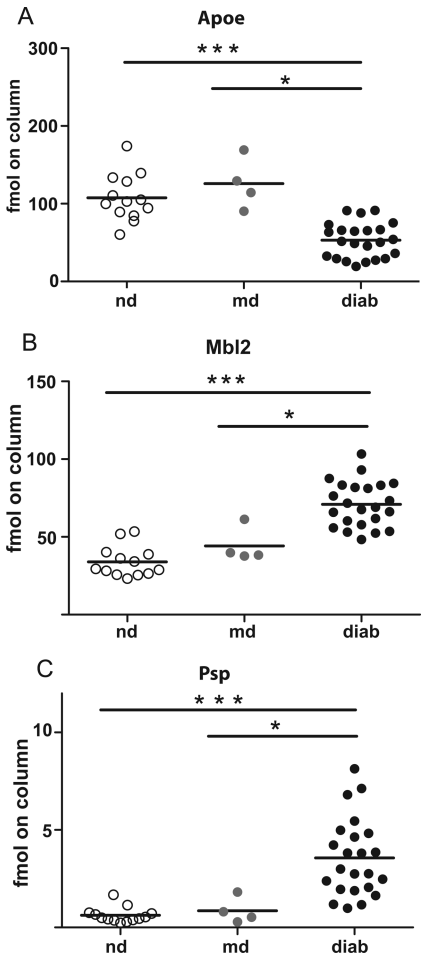


**Figure 4.** Absolute quantification using AQUA peptides. For absolute quantification two AQUA peptides for each of the three proteins Apoe (A), Mbl2 (B), and Psp (C) were used and concentrations calculated on the basis of the heavy (AQUA peptides) to light (endogenous peptide) ratios for the complete set of 40 animals (23 diabetic, 13 non-diabetic, and 4 moderately diabetic). A non-parametric ANOVA was performed comparing the animal groups with the Kruskal–Wallis test, followed by Dunn's post-test, correcting for multiple testing. The ANOVA demonstrated a highly statistical significance between the diabetic and the non-diabetic groups and a statistical significance between the non-diabetic and the moderately diabetic animals for all three proteins.

group. Similar to Mbl2, a higher concentration of Psp was detected in the diabetic animals. Again, statistical analysis demonstrated a high statistical significance between diabetics and non-diabetics ($p < 0.001$), as well as a statistical significance between the non-diabetic and the moderately diabetic animals ($p < 0.05$) (Figure 4C). All endogenous peptides were measured at concentrations above the LOQ of the respective assay (see Supplementary Table S8 and Supplementary Figure 3). Furthermore, the target protein with the lowest abundance in plasma was PSP with 30 ng/mL, which is well within detection limit of proteins measured in plasma using alternative depletion approaches and larger amounts of starting material.[34]

All absolute quantifications were in agreement with the relative quantifications and showed a closer resemblance of the moderately diabetic animals with the healthy non-diabetic animals than with the diabetic group.

### Validation of a Differential Mbl2 Concentration in Crude Plasma

To evaluate the influence of plasma depletion on the relative and absolute quantification of the candidate proteins, we quantified Mbl2 in non-depleted plasma samples using a direct ELISA. Mbl2 levels were directly measured by ELISA in 38 samples (23 diabetic, 12 non-diabetic, and 3 moderately diabetic) of the original non-depleted plasma samples used in this study. Quantification of Mbl2 in crude plasma confirmed the difference between the diabetic (3.5 pmol/$\mu$L crude plasma), the non-diabetic (2.3 pmol/$\mu$L crude plasma), and the moderately diabetic animals (3 pmol/$\mu$L) (Figure 5). Non-parametric ANOVA analysis followed by a post-test correcting for multiple testing demonstrated a statistical significance between the diabetic and the non-diabetic, but not to the moderately diabetic animals.

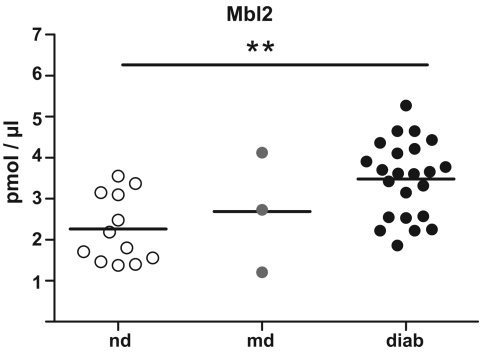


**Figure 5.** Mbl2 ELISA. A total of 38 (22 diabetic, 13 non-diabetic, and 3 moderately diabetic) of the original non-depleted plasma samples used for the mass spectrometric analysis were measured using a mouse Mbl2 ELISA. Quantification of Mbl2 in crude plasma demonstrated a highly significant difference between the diabetic and the non-diabetic group, but not to the moderately diabetic animals. For statistical analysis, a non-parametric ANOVA analysis was performed comparing the animal groups with the Kruskal–Wallis test, followed by Dunn's post-test, correcting for multiple testing. *P*-values less than 0.01 were considered to indicate statistically highly significant differences.

## DISCUSSION

### Quantitative Proteomics on ProteoMiner Depleted Mouse Plasma

The aim of this study was to establish a workflow that allowed proteomic profiling of limited amounts of plasma. This is of importance to a broad community not only because limited amounts of material are available from most animal models but also for epidemiological studies that have recently experienced a tremendous increase of importance because genome-wide SNP analyses are now routinely performed with large cohorts. In addition, the very high complexity of plasma proteomes requires depletion of highly abundant proteins in order to increase the depth of analysis. Highly abundant proteins such as albumin would not only mask low abundant proteins, but endogenous protease inhibitors might also prevent complete digestion of proteins, a prerequisite for correct proteomic quantification. Different depletion techniques have been developed over the years with varying success or outcome.[20,35] In a first step, we reviewed depletion methods with respect to their scalability. Bead-based depletion techniques often allow adjusting the amount of beads to available sample amounts, in


dx.doi.org/10.1021/pr3009836 | J. Proteome Res. 2013, 12, 1331–1343

contrast to antibody-based column depletion techniques. Next, the independence of taxonomy of a depletion approach is preferable, as this way a once established protocol can be easily adapted to other animal models, as well as human samples. Finally, when working with large numbers of samples such as epidemiological cohorts, an optimized depletion approach for high-throughput screenings is necessary.

Our depletion workflow resulted in a median interassay variability of 16% (CV), which is well comparable or even below the multisite assessment study by Addona et al.[33] or Kuzyk et al[28] that forego depletion of plasma in their studies and reach median with CVs of <15 and <20%, respectively. The most commonly used depletion methods are antibody-based depletions, which are very efficient for large sample input volumes and result in high numbers of identified proteins but also present with comparably high interassay variability. In their biomarker discovery studies, Addona et al. and Whiteaker et al. reach median CVs of 12−22% using different types of immunodepletion techniques.[4,36] With their electrophoretic sample preparation system, Harkins et al. present a depletion system adaptable to high throughput, with a CV of <30%,[37] almost twice the variation we could demonstrate for the ProteoMiner depletion approach. de Roos et al.[38] compared the Beckman Coulter IgY-12 proteome partitioning kit, the Amersham albumin and IgG depletion columns, and single-use immunoaffinity columns. The average within-laboratory CV for each of the matched spots after automatic matching using different software tools ranged between 18% and 69%, dependent on the cell type investigated. The higher reproducibility of our approach here as compared to antibody-based depletion may stem from the application of fresh beads for every sample while antibody-based depletion requires reusage of costly bead cartridges after washing and re-equilibration steps potentially affecting performance.

When comparing protein abundances between ProteoMiner depleted and crude plasma by label-free quantification, we found a reduction of 12 highly abundant proteins by more than 90%, including plasma albumin, transferrin, and haptoglobin (Table 1). Similar results were obtained by Polaskova et al.[39] comparing six different depletion columns by 2-DE. Comparing three multiple affinity columns, Yadav et al.[40] demonstrated depletion of >90% of the respective high abundant proteins of with this column-based approach; however, these columns also bind 48 unspecific proteins, affecting their proper quantification.[41−43] In summary, the protocol described here using ProteoMiner beads in a batch mode for small sample volumes facilitated an efficient depletion of highly abundant proteins with a high reproducibility. As our protocol is rapid and simple, it can be fully automated and could find future applications in large sample cohort studies to determine protein signatures that could complement metabolite analyses.[44]

As a proof of principle we applied our workflow to plasma from the NZO mouse model, screening for differentially abundant proteins associated with type 2 diabetes. To determine potential candidates, we used a shotgun proteomics approach with a test set of animals and chose 13 proteins for further validation in the targeted approach (SQ-SRM) using a large set of NZO mice. Validated by a SQ-SRM based principle component analysis, three candidate proteins were selected for further absolute quantification using the AQUA approach.[23] Prior to quantification, linear range, assay precision, and limits of detection and quantification were assessed. With a linear range of 3−4 orders of magnitude, a median assay precision of <20%, and limits of detection in the attomolar range, our assays corresponded well to the values reported by other groups.[4,33,34] The statistically significant differences between the concentrations of Apoe, Mbl2, and Psp from the SQ-SRM results could be confirmed by the absolute quantification, within the linear range for each assay and above the LOQ (Supplementary Table 3). While SQ-SRM only delivers ratios between protein abundances for each group, absolute quantification of candidates confirmed a difference in total abundance of the three candidate proteins between animal groups. While Apoe and Mbl2 are among the comparatively high expressed proteins in plasma and thus could also be detected in non-depleted plasma, Psp was only reliably detectible in PM-depleted plasma. Thus the detection and quantification of Psp also demonstrates that the PM-based depletion of highly abundant proteins efficiently enriches lower abundant ones.

To evaluate the influence of depletion on the quantification of the candidate proteins, we performed a direct ELISA-based measurement of the Mbl2 concentration in non-depleted plasma. The Mbl2 quantification in crude plasma using the ELISA technique confirmed the SRM-based relative quantifications of the depleted plasma samples. The Mbl2 ratios between the diabetic and the non-diabetic group in both techniques were almost indistinguishable, indicating that depletion of highly abundant proteins does not change relative proportions of proteins within the tested range.

## Candidates in the Context of T2D

Validated by absolute quantification, our proof of principle study on the NZO mouse model identified Apoe, Mbl2, and Psp to be differentially abundant between the diabetic and the non-diabetic groups of animals. While for Apoe lower concentrations associated with the diabetic phenotype, for Mbl2 and Psp higher concentrations did. Apolipoprotein E (Apoe) is a plasma lipoprotein synthesized in the liver. As the major apoprotein of the chylomicron, it binds to the cell surface LDL receptor and the chylomircon-remnant receptor on liver cells, as well as peripheral cells. There, it mediates the high-affinity binding of Apoe-containing lipoproteins. Apoe is an important mediator of transport and hepatic metabolic clearance of circulating cholesterol, further involved in the normal catabolism of triglyceride-rich lipoprotein constituents.[45−48] Dyslipidemia, diabetes, hypertension, and obesity are all risk factors for cardiovascular disease. The Apoe-deficient mouse displays hypercholesterolemia and spontaneously develops atherosclerosis.[49−51] More recent findings demonstrate that Apoe-deficient mice are also a model for the metabolic syndrome,[52] which is in accordance with the lower abundance of Apoe observed in our diabetic NZO mice compared to non-diabetic controls. Although the lipid profiles of mice and humans differ greatly, a role of Apoe in the context of atherosclerosis and T2D is also discussed in humans. In their study on patients with polycystic ovaries (PCO), Fan et al. suggest a connection between decreased levels of Apoe in patients and type 2 diabetes or future cardiovascular disease.[53]

The mannose-binding lectin (Mbl) proteins are recognition proteins of the lectin pathway. The lectin pathway belongs to the innate immune system and plays a role in complement activation, similar to the classical complement pathway.[54] Mbl2 shares a high degree of structural similarity with C1q, the initiating molecule of the classical pathway of complement activation.[55] Circulating Mbl2 protein is suggested to be a functional serum equivalent of the tissue macrophage mannose

receptor 2, and recognition of mannose-rich ligands in peripheral blood is conferred to liver-derived Mbl2.[56] Similarly to C1q and the mannose receptor, Mbl2 has been implicated in host defense[57] and the removal of apoptotic cells.[58] The role of Mbl2 in the context of ischemia and stroke-associated complement activation has been analyzed in experimental and human studies.[55] Our quantification of the Mbl2 plasma concentration in NZO mice showed a higher abundance of Mbl2 in diabetic animals, suggesting complement activation in those animals. This finding is in line with the observed protective effect of Mbl2-deficiency from acute ischemic stroke, recently identified in humans.[59,60] Interestingly, almost a third of the population worldwide suffers from functional Mbl2-deficiency, sometimes referred to as the most frequent human immunodeficiency.[61] It has been suggested that this high prevalence of mutations in the Mbl2 gene, resulting in low Mbl2 levels, could in some cases confer a biological advantage.[62] The study of Fortpied et al. not only examined the role of Mbl2 in the context of hyperglycemia and diabetes but also proposed a mechanism for complement activation in diabetes.[63] They state that the increase of fructosamine density on cell surfaces, as observed in diabetes, induces Mbl2 binding and hence activation of MASPs and other components of the complement cascade. Fortpied et al. observed that mice deficient in Mbl2 develop less diabetic nephropathy and cardiomyopathy, which argues in favor of a contribution of the lectin pathway in diabetic complications.[63] The higher abundance of Mbl2 in diabetic NZO is in coherence with this theory and presents Mbl2 as a potential pharmaceutical target. Although the exact mechanism leading to a higher Mbl2 plasma concentration in diabetic mice remains unknown, we aim to address this using additional mouse models in future studies.

Parotid secretory protein (Psp) is produced by the acinar cells of the parotid gland. It belongs to the palate, lung, and nasal epithelium clone (PLUNC) family of mucosal secretory proteins that are predicted to be structurally related to lipid-binding, host-defense, permeability-increasing, and lipopolysaccharide-binding proteins.[64] So far Psp has mainly been investigated in the saliva of rodent models and significant alterations in expression of different salivary proteins could be identified in rats with streptozotocin diabetes.[65] Only recently C20orf70 has been identified as a human homologue to the rodent Psp. Psp and the Plunc protein were identified as novel secretory proteins that are expressed in the oral cavity and upper airways.[66] A decreased concentration of Plunc was observed in the saliva of T2D patients.[67] Abdolhosseini et al. demonstrated that Psp is a lipopolysaccharide-binding protein, functionally related to LBP.[64] In rodents, Psp is associated with HDL, and the level of Psp in HDL was increased after endotoxin injection in hamsters, but not in mice.[68] Further, recombinant Psp appears to be a novel anticandidal protein associated with high-density lipoproteins, in culture.[68] The phospholipid-transfer protein (Pltp), a member of the PLUNC family of proteins, was one of our initial 13 candidates, tested for differential abundance between the diabetic and the non-diabetic animals. Pltp was less abundant in plasma diabetic, dyslipidemic animals but was not statistically significant due to a high variability in the non-diabetic group. Pltp was studied initially for its involvement in the HDL metabolism and reverse cholesterol transport.[69] Since Pltp can modulate the lipoprotein association and metabolism of LPS that are major components of Gram-negative bacteria, a pivotal role for Pltp in inflammation and innate immunity is discussed.[69] Through Pltp, Psp could be linked to other candidates differing in their abundance in our study. The association of Apoe and Psp with respect to lipoprotein transport and the association of Psp and Mbl2 as part of the innate immune system strengthen the connection of dyslipidemia and the innate immunity in T2D and relate alterations in plasma proteins in this diabesity mouse model to the human situation.

## CONCLUSION

Novel proteomic tools and strategies are required to complement genomic, transcriptomic, and metabolomic data from disease models. The presented analytical workflow facilitates quantitative proteomic analyses of limited samples amounts derived from animal models or biobank material. As a proof of principle, we identified phenotype-specific protein signatures in plasma of NZO mice that correspond to T2D-associated changes observed in humans. Cross validation of these candidate protein signatures in mouse models with a different genetic background but with the same T2D stages such as beta cell atrophy will help to dissect novel mechanisms besides the well-established changes.

## ASSOCIATED CONTENT

### Supporting Information

Supplementary tables and figures. This material is available free of charge via the Internet at http://pubs.acs.org.

## AUTHOR INFORMATION

### Corresponding Author

*E-mail: hauck@helmholtz-muenchen.de.

### Notes

The authors declare no competing financial interest.

## ACKNOWLEDGMENTS

We thank Silke Becker for her excellent technical assistance and Dr. Juliane Merl for constructive discussions. This work was supported by FKZ 03IS2061B Spitzenforschung und Innovation in den Neuen Ländern−GANI_MED−Greifswald Approach to Individualized Medicine PB1 1 Personalized Proteomics and by a grant from the German Federal Ministry of Education and Research (BMBF) to the German Center for Diabetes Research (DZD e.V.).

## ABBREVIATIONS

Amu, atomic mass unit; ANOVA, analysis of variance; Apoe, apolipoprotein E; AQUA, absolute quantification; AUC, area under the curve; CE, collision energy; CV, coefficient of variation; diab, diabetic; DTT, dithiothreitol; ELISA, enzyme-linked immunosorbent assay; fwhm, full width at half-maximum; LOD, limit of detection; LOQ, limit of quantification; MANOVA, multiple analyses of variances; Mbl2, mannose-binding lectin 2; md, moderately diabetic; MS, mass spectrometry; nd, non-diabetic; NZO, New Zealand Obese; PCA, principal component analysis; PM, ProteoMiner; Psp, parotid secretory protein; Pltp, phospholipid-transfer protein; RT, room temperature; SEM, standard error of the mean; SRM, selected reaction monitoring; T2D, type 2 diabetes; TR, technical reproducibility; v/v, volume to volume

## REFERENCES


(1) Hossain, P.; Kawar, B.; El Nahas, M. Obesity and diabetes in the developing world–a growing challenge. *N. Engl. J. Med.* **2007**, *356* (3), 213−215.

(2) Jurgens, H. S.; Neschen, S.; Ortmann, S.; Scherneck, S.; Schmolz, K.; Schuler, G.; Schmidt, S.; Bluher, M.; Klaus, S.; Perez-Tilve, D.; Tschop, M. H.; Schurmann, A.; Joost, H. G. Development of diabetes in obese, insulin-resistant mice: essential role of dietary carbohydrate in beta cell destruction. *Diabetologia* **2007**, *50* (7), 1481−1489.

(3) Poitout, V.; Robertson, R. P. Minireview: Secondary beta-cell failure in type 2 diabetes–a convergence of glucotoxicity and lipotoxicity. *Endocrinology* **2002**, *143* (2), 339−342.

(4) Whiteaker, J. R.; Lin, C.; Kennedy, J.; Hou, L.; Trute, M.; Sokal, I.; Yan, P.; Schoenherr, R. M.; Zhao, L.; Voytovich, U. J.; Kelly-Spratt, K. S.; Krasnoselsky, A.; Gafken, P. R.; Hogan, J. M.; Jones, L. A.; Wang, P.; Amon, L.; Chodosh, L. A.; Nelson, P. S.; McIntosh, M. W.; Kemp, C. J.; Paulovich, A. G. A targeted proteomics-based pipeline for verification of biomarkers in plasma. *Nat. Biotechnol.* **2011**, *29* (7), 625−634.

(5) Bielschowsky, F.; Bielschowsky, M. The New Zealand strain of obese mice; their response to stilboestrol and to insulin. *Aust. J. Exp. Biol. Med. Sci.* **1956**, *34* (3), 181−198.

(6) Crofford, O. B.; Davis, C. K., Jr. Growth characteristics, glucose tolerance and insulin sensitivity of New Zealand obese mice. *Metabolism* **1965**, *14*, 271−280.

(7) Junger, E.; Herberg, L.; Jeruschke, K.; Leiter, E. H. The diabetes-prone NZO/Hl strain. II. Pancreatic immunopathology. *Lab Invest.* **2002**, *82* (7), 843−853.

(8) Lange, C.; Jeruschke, K.; Herberg, L.; Leiter, E. H.; Junger, E. The diabetes-prone NZO/Hl strain. Proliferation capacity of beta cells in hyperinsulinemia and hyperglycemia. *Arch. Physiol. Biochem.* **2006**, *112* (1), 49−58.

(9) Thorburn, A.; Andrikopoulos, S.; Proietto, J. Defects in liver and muscle glycogen metabolism in neonatal and adult New Zealand obese mice. *Metabolism* **1995**, *44* (10), 1298−1302.

(10) Andrikopoulos, S.; Proietto, J. The biochemical basis of increased hepatic glucose production in a mouse model of type 2 (non-insulin-dependent) diabetes mellitus. *Diabetologia* **1995**, *38* (12), 1389−1396.

(11) Ortlepp, J. R.; Kluge, R.; Giesen, K.; Plum, L.; Radke, P.; Hanrath, P.; Joost, H. G. A metabolic syndrome of hypertension, hyperinsulinaemia and hypercholesterolaemia in the New Zealand obese mouse. *Eur. J. Clin. Invest.* **2000**, *30* (3), 195−202.

(12) McInerney, M. F.; Najjar, S. M.; Brickley, D.; Lutzke, M.; Abou-Rjaily, G. A.; Reifsnyder, P.; Haskell, B. D.; Flurkey, K.; Zhang, Y. J.; Pietropaolo, S. L.; Pietropaolo, M.; Byers, J. P.; Leiter, E. H. Anti-insulin receptor autoantibodies are not required for type 2 diabetes pathogenesis in NZL/Lt mice, a New Zealand obese (NZO)-derived mouse strain. *Exp. Diabesity. Res.* **2004**, *5* (3), 177−185.

(13) Jurgens, H. S.; Schurmann, A.; Kluge, R.; Ortmann, S.; Klaus, S.; Joost, H. G.; Tschop, M. H. Hyperphagia, lower body temperature, and reduced running wheel activity precede development of morbid obesity in New Zealand obese mice. *Physiol. Genomics* **2006**, *25* (2), 234−241.

(14) Leiter, E. H. Selecting the "right" mouse model for metabolic syndrome and type 2 diabetes research. *Methods Mol. Biol.* **2009**, *560*, 1−17.

(15) Kluge, R.; Giesen, K.; Bahrenberg, G.; Plum, L.; Ortlepp, J. R.; Joost, H. G. Quantitative trait loci for obesity and insulin resistance (Nob1, Nob2) and their interaction with the leptin receptor allele (LeprA720T/T1044I) in New Zealand obese mice. *Diabetologia* **2000**, *43* (12), 1565−1572.

(16) Reifsnyder, P. C.; Churchill, G.; Leiter, E. H. Maternal environment and genotype interact to establish diabesity in mice. *Genome Res.* **2000**, *10* (10), 1568−1578.

(17) Leiter, E. H.; Reifsnyder, P. C.; Flurkey, K.; Partke, H. J.; Junger, E.; Herberg, L. NIDDM genes in mice: deleterious synergism by both parental genomes contributes to diabetogenic thresholds. *Diabetes* **1998**, *47* (8), 1287−1295.

(18) Plum, L.; Giesen, K.; Kluge, R.; Junger, E.; Linnartz, K.; Schurmann, A.; Becker, W.; Joost, H. G. Characterisation of the mouse diabetes susceptibilty locus Nidd/SJL: islet cell destruction, interaction with the obesity QTL Nob1, and effect of dietary fat. *Diabetologia* **2002**, *45* (6), 823−830.

(19) Taylor, B. A.; Wnek, C.; Schroeder, D.; Phillips, S. J. Multiple obesity QTLs identified in an intercross between the NZO (New Zealand obese) and the SM (small) mouse strains. *Mamm. Genome* **2001**, *12* (2), 95−103.

(20) Anderson, N. L.; Anderson, N. G. The human plasma proteome: history, character, and diagnostic prospects. *Mol. Cell. Proteomics* **2002**, *1* (11), 845−867.

(21) Anderson, N. L. Counting the proteins in plasma. *Clin. Chem.* **2010**, *56* (11), 1775−1776.

(22) Boschetti, E.; Giorgio Righetti, P. Hexapeptide combinatorial ligand libraries: the march for the detection of the low-abundance proteome continues. *BioTechniques* **2008**, *44* (5), 663−665.

(23) Gerber, S. A.; Rush, J.; Stemman, O.; Kirschner, M. W.; Gygi, S. P. Absolute quantification of proteins and phosphoproteins from cell lysates by tandem MS. *Proc. Natl. Acad. Sci. U.S.A.* **2003**, *100* (12), 6940−6945.

(24) Fuchs, H.; Gailus-Durner, V.; Adler, T.; Aguilar-Pimentel, J. A.; Becker, L.; Calzada-Wack, J.; Da Silva-Buttkus, P.; Neff, F.; Gotz, A.; Hans, W.; Holter, S. M.; Horsch, M.; Kastenmuller, G.; Kemter, E.; Lengger, C.; Maier, H.; Matloka, M.; Moller, G.; Naton, B.; Prehn, C.; Puk, O.; Racz, I.; Rathkolb, B.; Romisch-Margl, W.; Rozman, J.; Wang-Sattler, R.; Schrewe, A.; Stoger, C.; Tost, M.; Adamski, J.; Aigner, B.; Beckers, J.; Behrendt, H.; Busch, D. H.; Esposito, I.; Graw, J.; Illig, T.; Ivandic, B.; Klingenspor, M.; Klopstock, T.; Kremmer, E.; Mempel, M.; Neschen, S.; Ollert, M.; Schulz, H.; Suhre, K.; Wolf, E.; Wurst, W.; Zimmer, A.; Hrabe de Angelis, M. Mouse phenotyping. *Methods* **2010**, *53* (2), 120−135.

(25) Gailus-Durner, V.; Fuchs, H.; Becker, L.; Bolle, I.; Brielmeier, M.; Calzada-Wack, J.; Elvert, R.; Ehrhardt, N.; Dalke, C.; Franz, T. J.; Grundner-Culemann, E.; Hammelbacher, S.; Holter, S. M.; Holzlwimmer, G.; Horsch, M.; Javaheri, A.; Kalaydjiev, S. V.; Klempt, M.; Kling, E.; Kunder, S.; Lengger, C.; Lisse, T.; Mijalski, T.; Naton, B.; Pedersen, V.; Prehn, C.; Przemeck, G.; Racz, I.; Reinhard, C.; Reitmeir, P.; Schneider, I.; Schrewe, A.; Steinkamp, R.; Zybill, C.; Adamski, J.; Beckers, J.; Behrendt, H.; Favor, J.; Graw, J.; Heldmaier, G.; Hofler, H.; Ivandic, B.; Katus, H.; Kirchhof, P.; Klingenspor, M.; Klopstock, T.; Lengeling, A.; Muller, W.; Ohl, F.; Ollert, M.; Quintanilla-Martinez, L.; Schmidt, J.; Schulz, H.; Wolf, E.; Wurst, W.; Zimmer, A.; Busch, D. H.; de Angelis, M. H. Introducing the German Mouse Clinic: open access platform for standardized phenotyping. *Nat. Methods* **2005**, *2* (6), 403−404.

(26) Hauck, S. M.; Dietter, J.; Kramer, R. L.; Hofmaier, F.; Zipplies, J. K.; Amann, B.; Feuchtinger, A.; Deeg, C. A.; Ueffing, M. Deciphering membrane-associated molecular processes in target tissue of autoimmune uveitis by label-free quantitative mass spectrometry. *Mol. Cell. Proteomics* **2010**, *9* (10), 2292−2305.

(27) Keller, A.; Nesvizhskii, A. I.; Kolker, E.; Aebersold, R. Empirical statistical model to estimate the accuracy of peptide identifications made by MS/MS and database search. *Anal. Chem.* **2002**, *74* (20), 5383−5392.

(28) Kuzyk, M. A.; Smith, D.; Yang, J.; Cross, T. J.; Jackson, A. M.; Hardie, D. B.; Anderson, N. L.; Borchers, C. H. Multiple reaction monitoring-based, multiplexed, absolute quantitation of 45 proteins in human plasma. *Mol. Cell. Proteomics* **2009**, *8* (8), 1860−1877.

(29) Boschetti, E.; Righetti, P. G. The art of observing rare protein species in proteomes with peptide ligand libraries. *Proteomics* **2009**, *9* (6), 1492−1510.

(30) Righetti, P. G.; Boschetti, E.; Zanella, A.; Fasoli, E.; Citterio, A. Plucking, pillaging and plundering proteomes with combinatorial peptide ligand libraries. *J. Chromatogr. A* **2010**, *1217* (6), 893−900.

(31) Mouton-Barbosa, E.; Roux-Dalvai, F.; Bouyssie, D.; Berger, F.; Schmidt, E.; Righetti, P. G.; Guerrier, L.; Boschetti, E.; Burlet-Schiltz, O.; Monsarrat, B.; Gonzalez de Peredo, A. In depth exploration of cerebrospinal fluid by combining peptide ligand library treatment and

label free protein quantification. *Mol. Cell. Proteomics* **2010**, *9* (5), 1006−1021.
(32) Merl, J.; Ueffing, M.; Hauck, S. M.; von Toerne, C. Direct comparison of MS-based label-free and SILAC quantitative proteome profiling strategies in primary retinal Muller cells. *Proteomics* **2012**, *12* (12), 1902−1911.
(33) Addona, T. A.; Abbatiello, S. E.; Schilling, B.; Skates, S. J.; Mani, D. R.; Bunk, D. M.; Spiegelman, C. H.; Zimmerman, L. J.; Ham, A. J.; Keshishian, H.; Hall, S. C.; Allen, S.; Blackman, R. K.; Borchers, C. H.; Buck, C.; Cardasis, H. L.; Cusack, M. P.; Dodder, N. G.; Gibson, B. W.; Held, J. M.; Hiltke, T.; Jackson, A.; Johansen, E. B.; Kinsinger, C. R.; Li, J.; Mesri, M.; Neubert, T. A.; Niles, R. K.; Pulsipher, T. C.; Ransohoff, D.; Rodriguez, H.; Rudnick, P. A.; Smith, D.; Tabb, D. L.; Tegeler, T. J.; Variyath, A. M.; Vega-Montoto, L. J.; Wahlander, A.; Waldemarson, S.; Wang, M.; Whiteaker, J. R.; Zhao, L.; Anderson, N. L.; Fisher, S. J.; Liebler, D. C.; Paulovich, A. G.; Regnier, F. E.; Tempst, P.; Carr, S. A. Multi-site assessment of the precision and reproducibility of multiple reaction monitoring-based measurements of proteins in plasma. *Nat. Biotechnol.* **2009**, *27* (7), 633−641.
(34) Surinova, S.; Schiess, R.; Huttenhain, R.; Cerciello, F.; Wollscheid, B.; Aebersold, R. On the development of plasma protein biomarkers. *J. Proteome Res.* **2012**, *10* (1), 5−16.
(35) Fonslow, B. R.; Carvalho, P. C.; Academia, K.; Freeby, S.; Xu, T.; Nakorchevsky, A.; Paulus, A.; Yates, J. R., 3rd Improvements in proteomic metrics of low abundance proteins through proteome equalization using ProteoMiner prior to MudPIT. *J. Proteome Res.* **2011**, *10* (8), 3690−700.
(36) Addona, T. A.; Shi, X.; Keshishian, H.; Mani, D. R.; Burgess, M.; Gillette, M. A.; Clauser, K. R.; Shen, D.; Lewis, G. D.; Farrell, L. A.; Fifer, M. A.; Sabatine, M. S.; Gerszten, R. E.; Carr, S. A. A pipeline that integrates the discovery and verification of plasma protein biomarkers reveals candidate markers for cardiovascular disease. *Nat. Biotechnol.* **2011**, *29* (7), 635−643.
(37) Harkins, J. B. t.; Katz, B. B.; Pastor, S. J.; Osucha, P.; Hafeman, D. G.; Witkowski, C. E.,, 2nd; Norris, J. L. Parallel electrophoretic depletion, fractionation, concentration, and desalting of 96 complex biological samples for mass spectrometry. *Anal. Chem.* **2008**, *80* (8), 2734−2743.
(38) de Roos, B.; Duthie, S. J.; Polley, A. C.; Mulholland, F.; Bouwman, F. G.; Heim, C.; Rucklidge, G. J.; Johnson, I. T.; Mariman, E. C.; Daniel, H.; Elliott, R. M. Proteomic methodological recommendations for studies involving human plasma, platelets, and peripheral blood mononuclear cells. *J. Proteome Res.* **2008**, *7* (6), 2280−2290.
(39) Polaskova, V.; Kapur, A.; Khan, A.; Molloy, M. P.; Baker, M. S. High-abundance protein depletion: comparison of methods for human plasma biomarker discovery. *Electrophoresis* **2010**, *31* (3), 471−482.
(40) Yadav, A. K.; Bhardwaj, G.; Basak, T.; Kumar, D.; Ahmad, S.; Priyadarshini, R.; Singh, A. K.; Dash, D.; Sengupta, S. A systematic analysis of eluted fraction of plasma post immunoaffinity depletion: implications in biomarker discovery. *PLoS One* **2011**, *6* (9), e24442.
(41) Stempfer, R.; Kubicek, M.; Lang, I. M.; Christa, N.; Gerner, C. Quantitative assessment of human serum high-abundance protein depletion. *Electrophoresis* **2008**, *29* (21), 4316−4323.
(42) Gong, Y.; Li, X.; Yang, B.; Ying, W.; Li, D.; Zhang, Y.; Dai, S.; Cai, Y.; Wang, J.; He, F.; Qian, X. Different immunoaffinity fractionation strategies to characterize the human plasma proteome. *J. Proteome Res.* **2006**, *5* (6), 1379−1387.
(43) Liu, T.; Qian, W. J.; Mottaz, H. M.; Gritsenko, M. A.; Norbeck, A. D.; Moore, R. J.; Purvine, S. O.; Camp, D. G.,, 2nd; Smith, R. D. Evaluation of multiprotein immunoaffinity subtraction for plasma proteomics and candidate biomarker discovery using mass spectrometry. *Mol. Cell. Proteomics* **2006**, *5* (11), 2167−2174.
(44) Suhre, K.; Shin, S. Y.; Petersen, A. K.; Mohney, R. P.; Meredith, D.; Wagele, B.; Altmaier, E.; Deloukas, P.; Erdmann, J.; Grundberg, E.; Hammond, C. J.; de Angelis, M. H.; Kastenmuller, G.; Kottgen, A.; Kronenberg, F.; Mangino, M.; Meisinger, C.; Meitinger, T.; Mewes, H. W.; Milburn, M. V.; Prehn, C.; Raffler, J.; Ried, J. S.; Romisch-Margl, W.; Samani, N. J.; Small, K. S.; Wichmann, H. E.; Zhai, G.; Illig, T.; Spector, T. D.; Adamski, J.; Soranzo, N.; Gieger, C. Human metabolic individuality in biomedical and pharmaceutical research. *Nature* **2011**, *477* (7362), 54−60.
(45) Breslow, J. L. Transgenic mouse models of lipoprotein metabolism and atherosclerosis. *Proc. Natl. Acad. Sci. U.S.A.* **1993**, *90* (18), 8314−8318.
(46) Plump, A. S.; Smith, J. D.; Hayek, T.; Aalto-Setala, K.; Walsh, A.; Verstuyft, J. G.; Rubin, E. M.; Breslow, J. L. Severe hypercholesterolemia and atherosclerosis in apolipoprotein E-deficient mice created by homologous recombination in ES cells. *Cell* **1992**, *71* (2), 343−353.
(47) Zhang, S. H.; Reddick, R. L.; Piedrahita, J. A.; Maeda, N. Spontaneous hypercholesterolemia and arterial lesions in mice lacking apolipoprotein E. *Science* **1992**, *258* (5081), 468−471.
(48) Mahley, R. W. Apolipoprotein E: cholesterol transport protein with expanding role in cell biology. *Science* **1988**, *240* (4852), 622−630.
(49) Osada, J.; Joven, J.; Maeda, N. The value of apolipoprotein E knockout mice for studying the effects of dietary fat and cholesterol on atherogenesis. *Curr. Opin. Lipidol.* **2000**, *11* (1), 25−29.
(50) Meir, K. S.; Leitersdorf, E. Atherosclerosis in the apolipoprotein-E-deficient mouse: a decade of progress. *Arterioscler., Thromb., Vasc Biol* **2004**, *24* (6), 1006−1014.
(51) Kolovou, G.; Anagnostopoulou, K.; Mikhailidis, D. P.; Cokkinos, D. V. Apolipoprotein E knockout models. *Curr. Pharm. Des.* **2008**, *14* (4), 338−351.
(52) King, V. L.; Hatch, N. W.; Chan, H. W.; de Beer, M. C.; de Beer, F. C.; Tannock, L. R. A murine model of obesity with accelerated atherosclerosis. *Obesity (Silver Spring)* **2010**, *18* (1), 35−41.
(53) Fan, P.; Liu, H.; Wang, Y.; Zhang, F.; Bai, H. Apolipoprotein E-containing HDL-associated platelet-activating factor acetylhydrolase activities and malondialdehyde concentrations in patients with PCOS. *Reprod. BioMed. Online* **2012**, *24* (2), 197−205.
(54) Wallis, R.; Mitchell, D. A.; Schmid, R.; Schwaeble, W. J.; Keeble, A. H. Paths reunited: Initiation of the classical and lectin pathways of complement activation. *Immunobiology* **2010**, *215* (1), 1−11.
(55) Osthoff, M.; Trendelenburg, G.; Eisen, D. P.; Trendelenburg, M. Mannose-binding lectin-the forgotten molecule? *Nat. Med.* **2011**, *17* (12), 1547−1548 ; author reply 1548.
(56) Ezekowitz, R. A.; Sastry, K.; Bailly, P.; Warner, A. Molecular characterization of the human macrophage mannose receptor: demonstration of multiple carbohydrate recognition-like domains and phagocytosis of yeasts in Cos-1 cells. *J. Exp. Med.* **1990**, *172* (6), 1785−1794.
(57) Eisen, D. P. Mannose-binding lectin deficiency and respiratory tract infection. *J. Innate Immun.* **2010**, *2* (2), 114−122.
(58) Ogden, C. A.; deCathelineau, A.; Hoffmann, P. R.; Bratton, D.; Ghebrehiwet, B.; Fadok, V. A.; Henson, P. M. C1q and mannose binding lectin engagement of cell surface calreticulin and CD91 initiates macropinocytosis and uptake of apoptotic cells. *J. Exp. Med.* **2001**, *194* (6), 781−795.
(59) Cervera, A.; Planas, A. M.; Justicia, C.; Urra, X.; Jensenius, J. C.; Torres, F.; Lozano, F.; Chamorro, A. Genetically-defined deficiency of mannose-binding lectin is associated with protection after experimental stroke in mice and outcome in human stroke. *PLoS One* **2010**, *5* (2), e8433.
(60) Osthoff, M.; Katan, M.; Fluri, F.; Schuetz, P.; Bingisser, R.; Kappos, L.; Steck, A. J.; Engelter, S. T.; Mueller, B.; Christ-Crain, M.; Trendelenburg, M. Mannose-binding lectin deficiency is associated with smaller infarction size and favorable outcome in ischemic stroke patients. *PLoS One* **2011**, *6* (6), e21338.
(61) Garred, P.; Larsen, F.; Seyfarth, J.; Fujita, R.; Madsen, H. O. Mannose-binding lectin and its genetic variants. *Genes Immun.* **2006**, *7* (2), 85−94.
(62) Ezekowitz, R. A. Genetic heterogeneity of mannose-binding proteins: the Jekyll and Hyde of innate immunity? *Am. J. Hum. Genet.* **1998**, *62* (1), 6−9.
(63) Fortpied, J.; Vertommen, D.; Van Schaftingen, E. Binding of mannose-binding lectin to fructosamines: a potential link between

hyperglycaemia and complement activation in diabetes. *Diabetes Metab. Res. Rev.* **2010**, *26* (4), 254−260.
(64) Abdolhosseini, M.; Sotsky, J. B.; Shelar, A. P.; Joyce, P. B.; Gorr, S. U. Human parotid secretory protein is a lipopolysaccharide-binding protein: identification of an anti-inflammatory peptide domain. *Mol. Cell. Biochem.* **2012**, *359* (1−2), 1−8.
(65) Mednieks, M. I.; Szczepanski, A.; Clark, B.; Hand, A. R. Protein expression in salivary glands of rats with streptozotocin diabetes. *Int. J. Exp. Pathol.* **2009**, *90* (4), 412−422.
(66) Geetha, C.; Venkatesh, S. G.; Bingle, L.; Bingle, C. D.; Gorr, S. U. Design and validation of anti-inflammatory peptides from human parotid secretory protein. *J. Dent. Res.* **2005**, *84* (2), 149−153.
(67) Border, M. B.; Schwartz, S.; Carlson, J.; Dibble, C. F.; Kohltfarber, H.; Offenbacher, S.; Buse, J. B.; Bencharit, S. Exploring salivary proteomes in edentulous patients with type 2 diabetes. *Mol. Biosyst.* **2012**, *8* (4), 1304−1310.
(68) Khovidhunkit, W.; Hachem, J. P.; Medzihradszky, K. F.; Duchateau, P. N.; Shigenaga, J. K.; Moser, A. H.; Movsesyan, I.; Naya-Vigne, J.; Kane, J. P.; Feingold, K. R.; Grunfeld, C. Parotid secretory protein is an HDL-associated protein with anticandidal activity. *Am. J. Physiol. Regul. Integr. Comp. Physiol.* **2005**, *288* (5), R1306−1315.
(69) Gautier, T.; Lagrost, L. Plasma PLTP (phospholipid-transfer protein): an emerging role in 'reverse lipopolysaccharide transport' and innate immunity. *Biochem. Soc. Trans.* **2011**, *39* (4), 984−988.